Direct top quark production at hadron colliders as a probe of new physics

M. Hosch, K. Whisnant, and B.-L. Young
Department of Physics and Astronomy, Iowa State University, Ames, Iowa 50011
(Received 31 March 1997)

We examine the effect of an anomalous flavor-changing chromomagnetic moment which allows direct top quark production (two partons combining into an unaccompanied single top quark in the s channel) at hadron colliders. We consider both t-c-g and t-u-g couplings. We find that the anomalous charm quark coupling parameter κ_c/Λ can be measured down to 0.06 TeV^{-1}(0.009 TeV^{-1}) at the Fermilab Tevatron with the Main Injector upgrade (CERN LHC). The anomalous up quark coupling parameter κ_u/Λ can be measured to 0.02 TeV^{-1}(0.003 TeV^{-1}) at the Tevatron (LHC). [S0556-2821(97)05119-9]

PACS number(s): 12.60.Cn, 14.65.Ha

INTRODUCTION

With the discovery of the top quark [1,2], the long anticipated completion of the fermion sector of the standard model has been achieved. Its unexpected large mass in comparison with the other known fermions suggests that the top quark may play a unique role in probing new physics, and has prompted both theorists and experimenters alike to search for anomalous couplings involving the top quark. On the experimental side, the Collider Detector at Fermilab (CDF) [3,4] and D0 [5] Collaborations have begun to explore the physics of top quark rare decays [3]. On the theoretical side, a systematic examination of anomalous top quark interactions, in a model-independent way, has been actively undertaken [6,7].

One possible set of anomalous interactions for the top quark is given by the flavor-changing chromomagnetic operators

$$\frac{\kappa_u}{\Lambda} g_s \overline{u} \sigma^{\mu\nu} \frac{\lambda^a}{2} t G^a_{\mu\nu} + \mathrm{H.c.} \tag{1}$$

and

$$\frac{\kappa_c}{\Lambda} g_s \overline{c} \sigma^{\mu\nu} \frac{\lambda^a}{2} t G^a_{\mu\nu} + \mathrm{H.c.}, \tag{2}$$

where Λ is the new physics scale, κ_c and κ_u define the strengths of the couplings, $G^a_{\mu\nu}$ is the gauge field tensor of the gluon, and g_s is the strong coupling constant. The investigation of these couplings is well motivated. Although these operators can be induced in the standard model through higher order loops, their effects are too small to be observable [8]. Therefore, any observed signal indicating these types of couplings is direct evidence for physics beyond the standard model.

It has been argued that the couplings in Eqs. (1) and (2) may be significant in many extensions to the standard model, such as supersymmetry (SUSY) or other models with multiple Higgs doublets [8–11], models with new dynamical interactions of the top quark [12], and models where the top quark has a composite [13] or soliton [14] structure. In particular, Ref. [10] suggests that the supersymmetric contributions to a t-c-g vertex may be large enough to measure at a future hadron collider.

Han *et al.* [15] have placed a limit on the top-quark–charm-quark–gluon coupling strength κ_c by examining the decay of the top quark into a charm quark and a gluon. They find that an upper limit on κ_c/Λ of 0.43(0.65) TeV^{-1} with (without) b tagging for 200 pb^{-1} of data can be measured at the Tevatron. If the c and u jets are not distinguished, their result applies equally well to κ_u/Λ, if one uses the up quark coupling alone, or to the sum, added in quadrature, when both are considered.

In this paper, we will examine these operators in a model-independent way using direct top quark production at the Fermilab Tevatron and at the CERN Large Hadron Collider (LHC). In this scenario, a charm (or up) quark and a gluon from the colliding hadrons combine immediately to form an s-channel top quark, which then decays. The production of a single, unaccompanied top quark or top antiquark is very small in the standard model. We will take as our signal only the case where the top quark decays to a b quark and a W boson. While the $t \to cg$ (or ug) decay will occur in the presence of the anomalous couplings given in Eqs. (1) and (2), it is smaller than the $t \to bW$ decay for $\kappa/\Lambda \lesssim 0.75\ \mathrm{TeV}^{-1}$, and will have a negligible branching ratio for $\kappa/\Lambda \lesssim 0.2\ \mathrm{TeV}^{-1}$. Given the existing upper bound of the anomalous coupling mentioned earlier [15], $t \to bW$ will be the dominant decay mode of the top quark. Since the W boson decay into a charged lepton (electron or muon) and its corresponding neutrino has an identifiable signature, we con-

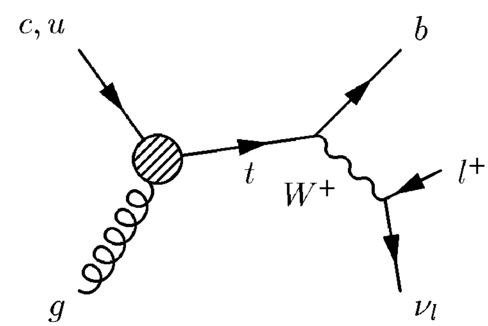

FIG. 1. Feynmann diagram for direct top quark production and subsequent decay into $b l \nu_l$.

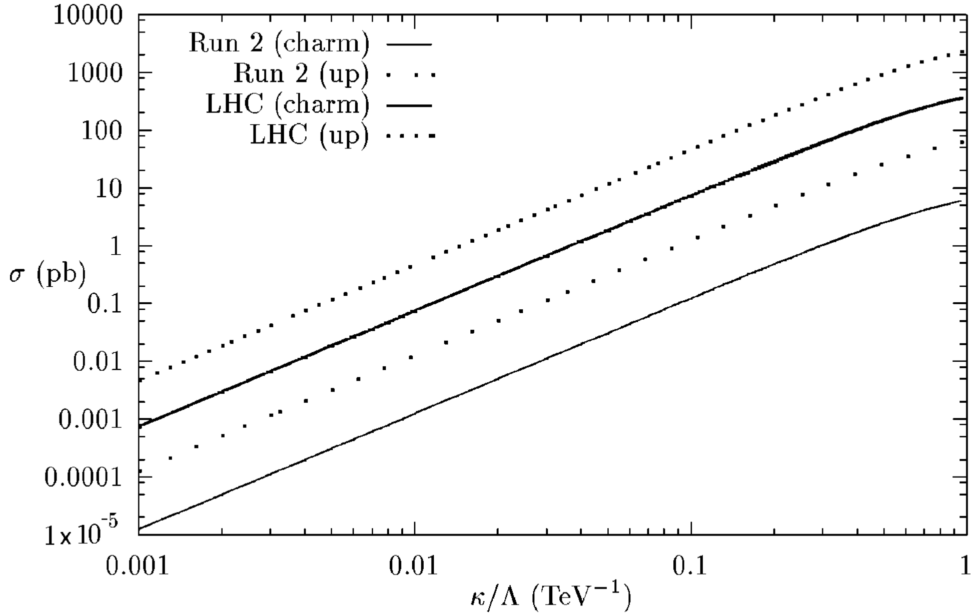

FIG. 2. Direct top quark cross section vs κ/Λ at run 2 of the Tevatron and the LHC. The cross sections for run 1 of the Tevatron are barely distinguishable from run 2, and are not shown here.

sider only the $t\to bW\to bl\nu_l$ decay for our signal. With the decays so chosen, we find that the backgrounds are manageable, as will be discussed in detail later.

DIRECT TOP QUARK PRODUCTION

We have calculated tree level cross sections for direct top quark production, $p\bar{p}\to t\to bW^+\to bl^+\nu_l$, using the flavor-changing chromomagnetic moments in Eqs. (1) and (2) (see Fig. 1). The l^+ in this process is either a positron or an antimuon, and ν_l is its corresponding neutrino. We also included direct top antiquark production in our calculation ($p\bar{p}\to\bar{t}\to\bar{b}W^-\to\bar{b}l^-\bar{\nu}_l$). The parton cross section for direct top quark (or top antiquark) production is given by

$$d\sigma=\frac{1}{4}\frac{1}{(4\pi)^5}\frac{\hat{s}-M^2_{l,\nu_l}}{\hat{s}^2}|\overline{\mathcal{M}}|^2 d\Omega_b d\Omega_l dM^2_{l,\nu_l}, \tag{3}$$

where the spin-averaged squared matrix element is

$$|\overline{\mathcal{M}}|^2=\frac{256\pi^3\alpha^2\alpha_s}{3\sin^4\theta_W}\frac{\kappa^2_{c(u)}}{\Lambda^2}\times\frac{\hat{s}(p_b\cdot p_{\nu_l})[\hat{s}(q_{c(u)}\cdot p_l)+m_t^2(q_g\cdot p_l)]}{[(\hat{s}-m_t^2)^2+m_t^2\Gamma_t^2][(M^2_{l,\nu_l}-M_W^2)^2+M_W^2\Gamma_W^2]}, \tag{4}$$

p_{b,l,ν_l} are the four-momenta of the outgoing b quark, lepton, and neutrino, respectively, $q_{c(u),g}$ are the four-momenta of the incoming charm (up) quark and gluon, Γ_W is the decay width of the W boson,

$$\Gamma_t=\Gamma_{t\to bW}\left[1+\frac{128M_W^2\alpha_s}{3\alpha_2\left(1-M_W^2/m_t^2\right)^2\left(1+2M_W^2/m_t^2\right)}\times\left(\frac{\kappa_c^2+\kappa_u^2}{\Lambda^2}\right)\right] \tag{5}$$

is the decay width of the top quark, including the anomalous contribution for $t\to cg$ and $t\to ug$, $\Gamma_{t\to bW}$ is the standard model top quark decay width to a b quark and W boson,

$$M^2_{l,\nu_l}\equiv(p_l+p_{\nu_l})^2 \tag{6}$$

is the invariant mass squared, not necessarily on shell, of the W boson, and $\sqrt{\hat{s}}$ is the parton center-of-mass energy.

As mentioned earlier, we considered only the case which has a charged lepton (muon or electron) in the final state, to identify the W boson. Compared to the hadronic decay mode of the W, the background for these processes is smaller and the signal is not as hard to identify. In order to examine the kinematics of the decay products, we calculated the full three-body phase space for the process, using the Breit-Wigner propagators to broaden the top quark and W boson distributions. Figure 2 shows the cross section at the Tevatron and LHC as a function of κ/Λ. In the top quark decay width, we included an additional term arising from $t\to c(u)g$, as shown in Eq. (5). This term is proportional to $|\kappa/\Lambda|^2$ and contributes significantly to the top quark width only if $\kappa/\Lambda\gtrsim0.2$ TeV^{-1}. One can see the effect of the additional channel for top quark decay, which decreases the $t\to bW$ branching ratio and causes a noticeable deviation from quadratic behavior for $\kappa/\Lambda\gtrsim0.2$ TeV^{-1}. (For $\kappa/\Lambda\gtrsim0.2$ there is a deviation from the straight line that one would expect on a log-log plot if the cross section scaled quadratically.)

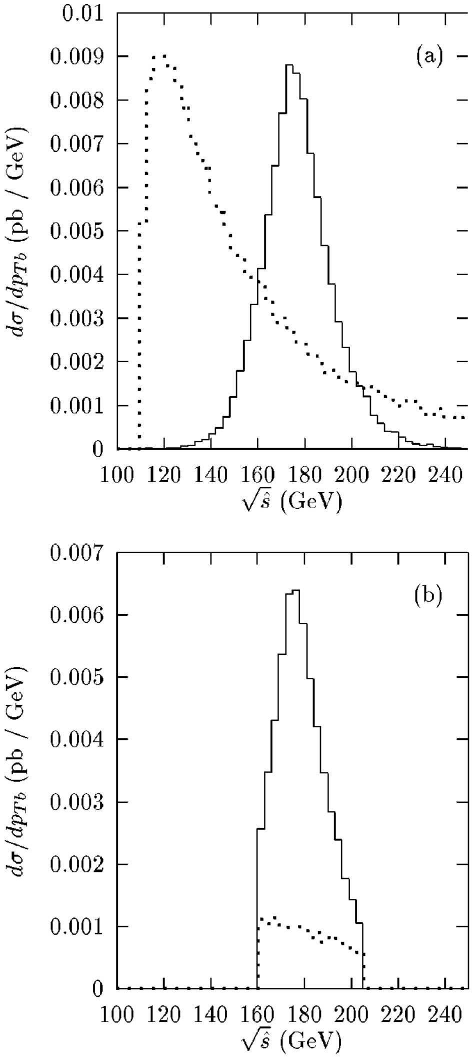

FIG. 3. $\sqrt{\hat{s}}$ distributions for the (a) basic and (b) optimized cuts without b tagging at the upgraded Tevatron. The solid line represents the direct top quark production ($\kappa_c/\Lambda = 0.2\ \mathrm{TeV}^{-1}$). The dotted line is one thousandth of the $W+1$ jet background.

We calculated the $p\overline{p}$ (for the Tevatron) and pp (for the LHC) cross sections for direct top quark production with the Martin-Roberts-Stirling set A (MRSA) structure functions [16]. We have also examined the effect of using the CTEQ3M [17] structure functions. The difference between the two sets of structure functions is small. Several distributions were calculated, including the transverse momenta, the pseudorapidities, the jet separation, from the lepton, and the reconstructed $\sqrt{\hat{s}}$.

In order to reduce the $W+1$ jet background, we made a series of cuts, which we will call the basic cuts, on the kinematic distributions. They are

$$p_T(b,l,\nu_l) \geqslant 25\ \mathrm{GeV}, \tag{7}$$

$$\eta_b \leqslant 2.0, \tag{8}$$

$$\eta_l \leqslant 3.0, \tag{9}$$

$$\Delta R \geqslant 0.4, \tag{10}$$

where $\eta_{b,l}$ are the pseudorapidities, $\Delta R \equiv \sqrt{(\eta_b-\eta_l)^2+(\phi_b-\phi_l)^2}$ is the separation between the b jet and the charged lepton in the detector, and $\phi_{b,l}$ are the azimuthal angles. We also assumed a Gaussian smearing of the energy of the final state particles, given by

$$\Delta E/E = 30\%/\sqrt{E} \oplus 1\% \quad \text{for leptons}, \tag{11}$$

$$= 80\%/\sqrt{E} \oplus 5\% \quad \text{for hadrons}, \tag{12}$$

where $\oplus$ indicates that the energy-dependent and -independent terms are added in quadrature.

To enhance the signal relative to the background, we want to make cuts on $\sqrt{\hat{s}}$, which should be sharply peaked at m_t for the signal. To experimentally determine $\sqrt{\hat{s}}$, one must reconstruct $p_t = p_b + p_l + p_{\nu_l}$. The neutrino is not observed, but its transverse momentum can be deduced from the missing transverse momentum. The longitudinal component of the neutrino momentum is determined by setting $M_{l,\nu_l} = M_W$ in Eq. (6), and is given by

$$p_L^{\nu_l} = \frac{\chi p_L^l \pm \sqrt{\vec{p}_l^{\,2}(\chi^2 - p_{Tl}^2 p_{T\nu_l}^2)}}{p_{Tl}^2}, \tag{13}$$

where

$$\chi = \frac{M_W^2}{2} + \vec{p}_T^{\,l} \cdot \vec{p}_T^{\,\nu_l}, \tag{14}$$

and p_L and p_T refer to the longitudinal and transverse momenta, respectively. Note that there is a twofold ambiguity in this determination. We chose the solution which would best reconstruct the mass of the top quark. In some rare cases, the quantity under the square root in Eq. (13) is negative due to the smearing discussed above. When this happened, we set this square root to zero, and used the corresponding result for the neutrino longitudinal momentum.

BACKGROUND CALCULATION

The main source of background to the direct top quark production is $p\overline{p} \to W+1$ jet. Another background process is standard model single top quark production when the associated jets are not observed. Examining the data presented in Ref. [18], we conclude that single top quark production is less than 1% of the $W+1$ jet background when b tagging is not used. When b tagging reduces the $W+1$ jet background by a factor of 100, the single top quark background may be as large as 20% of the total background. However, since the discovery limit on κ/Λ scales as $B^{-1/4}$ where B is the number of background events, a 20% change in the background affects the discovery limit by only 5%. We therefore ignore this background.

We used the VECBOS Monte Carlo [19] program to calculate the cross section for the $W+1$ jet background. We modified the program to produce the same distributions that were calculated for the signal, and applied the same basic cuts used in the signal calculation, Eqs. (7)–(10). To determine additional cuts which optimize the discovery limits on κ/Λ,

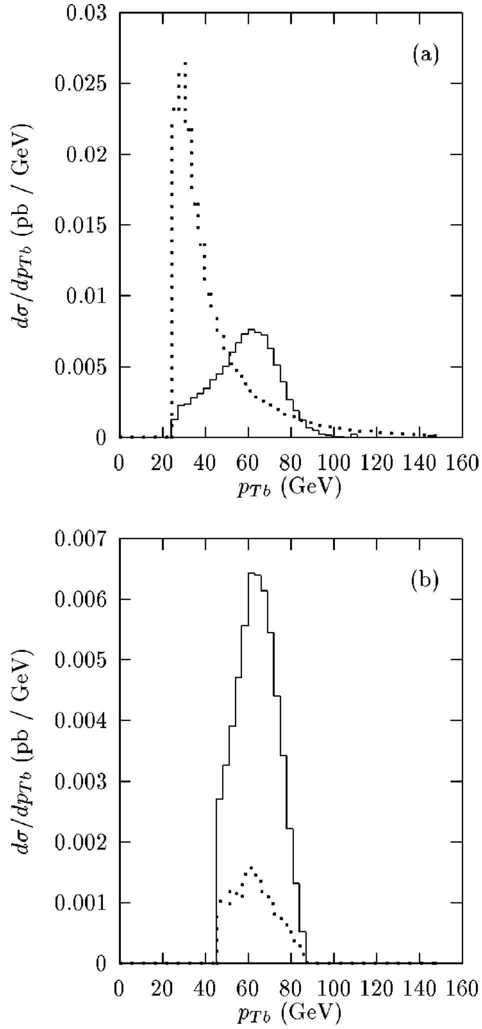

FIG. 4. p_{Tb} distributions for the (a) basic and (b) optimized cuts without b tagging at the upgraded Tevatron. The solid line represents the direct top quark production ($\kappa_c/\Lambda = 0.2$ TeV^{-1}). The dotted line is one thousandth of the $W+1$ jet background.

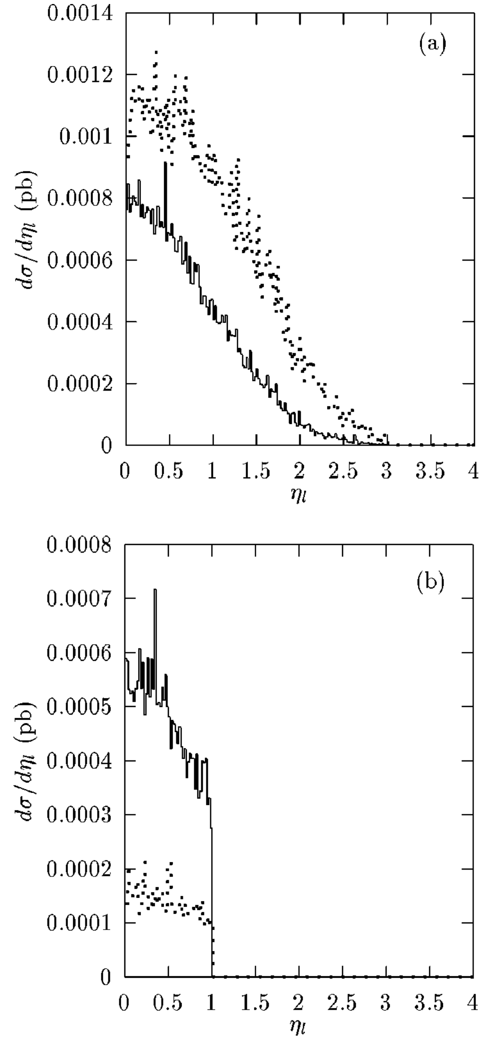

FIG. 5. η_l distributions for the (a) basic and (b) optimized cuts without b tagging at the upgraded Tevatron. The solid line represents the direct top quark production ($\kappa_c/\Lambda = 0.2$ TeV^{-1}). The dotted line is one thousandth of the $W+1$ jet background.

we examined the kinematic distributions in $\sqrt{\hat{s}}$, p_T, η, and ΔR. We found that three distributions, $\sqrt{\hat{s}}$, p_{Tb}, and η_l, were most useful in isolating the signal from the background. These are shown in Figs. 3, 4, and 5, with the charm quark in the initial state and $\kappa_c/\Lambda = 0.2$ TeV for the upgraded Tevatron. The solid lines represent direct top quark production, and the dashed lines represent the $W+1$ jet background divided by 1000. The cuts were optimized for each of four cases: run 1 at the Tevatron with $p\bar{p}$ collisions at $\sqrt{s} = 1.8$ TeV and 100 pb^{-1} of data per detector, run 2 with $\sqrt{s} = 2.0$ TeV and 2 fb^{-1}, run 3 with 2.0 TeV and 30 fb^{-1}, and the LHC with pp collisions at 14 TeV and 10 fb^{-1}. The optimized cuts are shown in Table I. The corresponding distributions with the up quark in the initial state are not shown; they have the same shape as for the charm quark, but are a factor of 10 larger in magnitude, due to the much larger size of the valence up quark distribution in the initial state.

To further reduce the background, we assumed that silicon vertex tagging of the b jet would be available, with 36% efficiency at run 1 of the Tevatron, and 60% at runs 2 and 3, and at the LHC. In addition, we assumed that 1% of all non-b-quark jets would be mistagged as b quark jets.

When b tagging is present, if the jet produced is mistaken as a b jet, it remains a part of the background. The background can be reduced by a factor of 100 if the $W+1$ jet sample does not include a significant fraction of b quarks in the final state. It is possible to estimate the fraction of b quarks in the $W+1$ jet sample by taking the ratio $|V_{cb}|^2/|V_{ud}|^2$ and multiplying by the ratio of the distribution fraction of charm quarks to up quarks in the proton, $0.2-0.005$ $(0.7-0.05)$, in the momentum fraction region where most of the events occur for the Tevatron (LHC). We

TABLE I. Optimized cuts for direct top quark production.

	$E_{\text{C.M.}}$ [TeV]	$(p_{Tb})_{\min}$ [GeV]	$(\sqrt{\hat{s}})_{\min}$	$(\sqrt{\hat{s}})_{\max}$	$(\eta_l)_{\max}$
Run 1	1.8	35	155 GeV	205 GeV	1.8
Run 2	2.0	45	160 GeV	205 GeV	1.0
Run 3	2.0	45	160 GeV	205 GeV	1.0
LHC	14.0	35	165 GeV	195 GeV	1.0

TABLE II. Signal needed for the discovery of anomalous t-c-g and t-u-g couplings at the Tevatron and LHC at 95% confidence level. The background cross sections use the optimized cuts described in Table I.

	$\sqrt{s}$ TeV	Luminosity (fb^{-1})	Background (fb)	Signal needed (fb) Without b tag	With b tag
Run 1	1.8	0.1	19400	1370	190
Run 2	2.0	2	13000	245	27
Run 3	2.0	30	13000	63	6.4
LHC	14	10	79000	267	27

TABLE III. Discovery limits on κ_c/Λ (with $\kappa_u=0$) and κ_u/Λ (with $\kappa_c=0$) at the Tevatron and LHC. The results are reported in TeV^{-1}.

		Tevatron			LHC
		1.8 TeV	2 TeV		14 TeV
	b tagging?	0.1 fb^{-1}	2 fb^{-1}	30 fb^{-1}	10 fb^{-1}
Charm	no	0.38	0.14	0.073	0.020
	yes	0.22	0.062	0.030	0.0084
u quark	no	0.096	0.045	0.023	0.0081
	yes	0.058	0.019	0.0094	0.0033

estimate that the fraction of b quark jets in the $W+1$ jet background is less than 0.03% (0.12%), much less than the anticipated mistagging rate of 1%. We therefore ignore the possibility of having b quarks in the $W+1$ jet sample. Including b tagging does not significantly affect the optimized cuts.

RESULTS AND DISCUSSION

We can use the results of the signal and background calculations to determine the minimum value of κ_c/Λ or κ_u/Λ observable at hadron colliders. Assuming Poisson statistics, the number of signal events (S) required for discovery of a signal at the 95% confidence level is

$$\frac{S}{\sqrt{S+B}} \geqslant 3, \tag{15}$$

where B is the number of background events obtained by multiplying the background cross section by the luminosity and dividing by 100 if b tagging is present. The luminosity, background cross section, and signal cross section needed for discovery of anomalous flavor-changing couplings are given in Table II. The discovery limits may then be determined by comparing the signal calculation for a given κ/Λ to the signal needed, which can be obtained from Table II. These discovery limits are shown in Table III.

Because the charm and up quarks are in the initial state, their contributions to direct top quark production cannot be distiguished. A plot of the discovery limit when both κ_c and κ_u are assumed to be nonzero is shown in Fig. 6.

The results quoted in this paper all use the MRSA structure functions. When using the CTEQ3M structure functions, the direct top quark cross section increases by 15% when the charm quark coupling is used, corresponding to a 7% decrease in the discovery limit for κ_c/Λ. This is primarily due to a larger charm quark density in the proton with the CTEQ3M structure functions. The $W+1$ jet cross section does not change significantly, nor does the direct top quark cross section when the up quark coupling is used. This difference reflects our lack of understanding of the charm quark distibution in the proton. Ultimately, this effect will be part of the theoretical uncertainty in the measured value of κ_c.

We considered cases with and without b tagging for each of the possibilities in Table III. With the exception of run 1 at the Tevatron, b tagging improved the discovery limit on κ/Λ by 2.0–2.5 times. However, for the data from run 1 at the Tevatron, b tagging improves the discovery limit by only

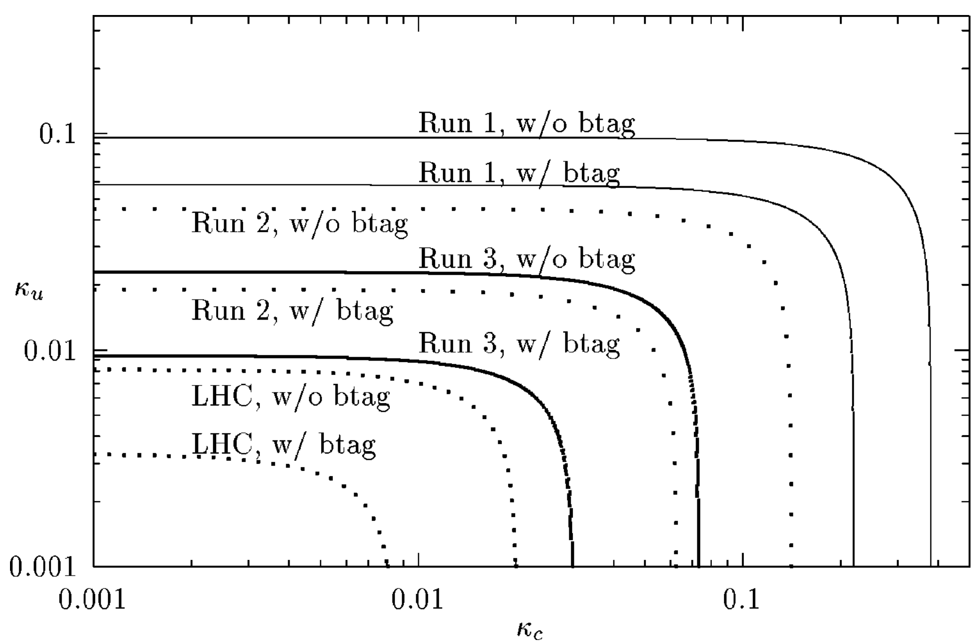

FIG. 6. Discovery limits for κ_c and κ_u for each of the colliders considered, for $\Lambda=1$ TeV.

40%. This is mostly due to less efficient b tagging and to the smaller number of events available with a lower luminosity.

In some single top quark production processes, there are regions of overlap between, for example, $2\to1$ subprocesses and $2\to2$ subprocesses. In particular, we worried about an overlap between the direct top quark production and the gluon fusion diagram in which one of the gluons is dissociated into a $c\bar{c}$ pair, and the c combines with the other gluon to produce a top quark. Care must be taken with these processes to avoid double counting. A systematic method exists for calculating a subtraction term which solves this difficulty [18,20]. The effect of the double counting is most significant if the initial state particles are massive. In the case of direct top quark production due to anomalous t-c-g or t-u-g couplings, the initial state particles are light enough that this does not significantly affect the overall cross section. We have therefore ignored this effect in our calculation.

Although the background due to single top quark production (a top quark with an associated jet) is small in the SM, there exists also the possibility for single top quark production with the anomalous t-c-g (or t-u-g) coupling [21], e.g., via $q\bar{q}\to t\bar{c}$ $(q\bar{q}\to t\bar{u})$. If the jet associated with the top quark is not seen, this would enhance the direct top quark signal due to the anomalous coupling. Therefore, the discovery limits quoted in Table III are conservative estimates of the level to which κ/Λ may be probed. A full treatment of single top quark production due to the anomalous t-c-g and t-u-g couplings will be considered elsewhere.

In conclusion, we have calculated the discovery limits for the anomalous chromomagnetic couplings t-c-g and t-u-g in hadron colliders using direct production of an s-channel top quark. We conservatively estimate that an anomalous charm quark coupling can be detected down to $\kappa_c/\Lambda=0.06\ \mathrm{TeV}^{-1}$ at run 2 of the Tevatron and $0.009\ \mathrm{TeV}^{-1}$ at the LHC. The cross section for the anomalous up quark coupling is larger, and we can measure κ_u/Λ down to $0.02\ \mathrm{TeV}^{-1}$ at run 2 of the Tevatron and $0.003\ \mathrm{TeV}^{-1}$ at the LHC. The discovery limits for the upgraded Tevatron are approximately 2 (6) times better than those obtained in Ref. [15] for κ_c/Λ (κ_u/Λ). The relative size of the direct top quark production and the anomalous top quark decay rate will help to differentiate the t-c-g and the t-u-g couplings.

Finally, we note that, in Ref. [10], the authors found that electroweaklike corrections in a supersymmetric model can give $B(t\to cg)$ as large as 1×10^{-5} for the most favorable combinations of the parameters. In terms of our anomalous coupling parameter, this corresponds to $\kappa_c/\Lambda=0.0033$. If supersymmetry is the only source for the anomalous t-c-g coupling, our calculations therefore indicate that future improvements at the LHC will be needed to make this a detectable signal, unless QCD-like corrections [9] further enhance the SUSY contributions, as discussed in Ref. [10].

ACKNOWLEDGMENTS

We would like to thank P. Baringer, T. Han, J. Hauptman, A. Heinson, T. LeCompte, and X. Zhang for many useful discussions. This work was supported in part by the U.S. Department of Energy under Contract No. DE-FG02-94ER40817. M.H. was also supported by GAANN.

[1] F. Abe *et al.*, Phys. Rev. Lett. **74**, 2626 (1995).
[2] S. Abachi *et al.*, Phys. Rev. Lett. **74**, 2632 (1995).
[3] J. Incandela, Nuovo Cimento A **109**, 741 (1996).
[4] Thomas J. LeCompte, FERMILAB-CONF-96-021-E, 1996.
[5] A.P. Heinson, *Future Top Physics at the Tevatron and LHC*, Proceedings of the QCD and high energy hadronic interactions, Les Arcs, 1996 (Editions Frontières, Gif-sur-Yvette, France, 1996), pp. 43–52.
[6] T. Han, K. Whisnant, B. L. Young, and X. Zhang, Phys. Rev. D **55**, 7241 (1997); K. Whisnant, Jin-Min Yang, Bing-Lin Young, and X. Zhang, *ibid.* **56**, 467 (1997); R. Martinez and J-Alexis Rodriguez, *ibid.* **55**, 3212 (1997).
[7] D. Atwood, A. Kagan, and T.G. Rizzo, Phys. Rev. D **52**, 6264 (1995); Douglas O. Carlson, Ehab Malkawi, and C.P. Yuan, Phys. Lett. B **337**, 145 (1994); G.J. Gounaris, M. Kuroda, and F.M. Renard, Phys. Rev. D **54**, 6861 (1996); G.J. Gounaris, J. Layssac, and F.M. Renard, *ibid.* **55**, 5786 (1997).
[8] B. Grzadkowski, J.F. Gunion, and P. Krawczyk, Phys. Lett. B **268**, 106 (1991); G. Eliam, J.L. Hewett, and A. Soni, Phys. Rev. D **44**, 1473 (1991); M. Luke and M.J. Savage, Phys. Lett. B **307**, 387 (1993).
[9] G. Couture, C. Hamzaoui, and H. König, Phys. Rev. D **52**, 1713 (1995).
[10] Jorge L. Lopez, D.V. Nanopoulos, and Raghavan Rangarajan, Phys. Rev. D **56**, 3100 (1997).
[11] T.P. Cheng and M. Sher, Phys. Rev. D **48**, 3484 (1987); W.S. Hou, Phys. Lett. B **296**, 179 (1992); L.J. Hall and S. Weinberg, Phys. Rev. D **48**, 979 (1993); D. Atwood, L. Reina, and A. Soni, *ibid.* **53**, 1199 (1996).
[12] C.T. Hill, Phys. Lett. B **266**, 419 (1991); **345**, 483 (1995); B. Holdom, *ibid.* **339**, 114 (1994); **351**, 279 (1995).
[13] H. Georgi, L. Kaplan, D. Morin, and A. Schenk, Phys. Rev. D **51**, 3888 (1995); for a review of composite models, see, e.g., R.D. Peccei, in *Proceedings of the 1987 Lake Louise Winter Institute: Selected Topics in the Electroweak Interactions*, edited by J.M. Cameron *et al.* (World Scientific, Singapore, 1987).
[14] X. Zhang, Phys. Rev. D **51**, 5309 (1995); J. Berger, A. Blotz, H.-C. Kim, and K. Goeke, *ibid.* **54**, 3598 (1996).
[15] T. Han, K. Whisnant, B.-L. Young, and X. Zhang, Phys. Lett. B **385**, 311 (1996).
[16] A.D. Martin, R.G. Roberts, and W.J. Stirling, Phys. Rev. D **50**, 6734 (1994).
[17] H.L. Lai, J. Botts, J. Huston, J.G. Morfin, J.F. Owens, J. Qiu, W.K. Tung, and H. Weerts, Phys. Rev. D **51**, 4763 (1995).
[18] A.P. Heinson, A.S. Belyaev, and E.E. Boos, Phys. Rev. D **56**, 3114 (1997).
[19] F.A. Berends, H. Kuijf, B. Tausk, and W.T. Giele, Nucl. Phys. **B357**, 32 (1991).
[20] R.M. Barnett, H.E. Haber, and D.E. Soper, Nucl. Phys. **B306**, 697 (1988); F.W. Olness and W.-K. Tung, *ibid.* **B308**, 813 (1988).
[21] E. Malkawi and T. Tait, Phys. Rev. D **54**, 5758 (1996).